Joint Center for Satellite Data Assimilation

Office Note CRTM-5

CRTM: Himawari-8/9 AHI Spectral Response Function Processing

Paul van Delst[a]
NCEP/EMC/IMSG

March 7, 2016; rev71462

---

[a]paul.vandelst@noaa.gov

Change History

Date	Author	Change
2016-03-07	Paul van Delst	Initial release.

Contents

List of Figures

List of Tables

1 Introduction

This document describes the pre-processing applied to the Himawari-8 and -9 platform Advanced Himawari Imager (AHI) spectral response functions (SRFs), obtained from JMA/MSC [a,b], to prepare for use in the CRTM processing chain. The SRFs are used to generate channel central frequencies, as well as in the convolution of monochromatic quantities such as Planck radiances or line-by-line (LBL) model generated transmittances to produce such things as polychromatic correction coefficients and instrument resolution transmittances. The latter, for a diverse set of atmospheric profiles, are then regressed against a set of predictors to produce the fast transmittance model coefficients used by the CRTM.

1.1 Computation of the channel central frequency

The computed AHI channel central frequencies, ν_0, are the first moments of the defined SRF,

$$\nu_0 = \frac{\int \nu\, \phi_{rel}(\nu)\, \mathrm{d}\nu}{\int \phi_{rel}(\nu)\, \mathrm{d}\nu} \tag{1.1}$$

For multiple passband channels, each band is numerically integrated and summed to give the total. It should also be noted that all calculations (in the SRF processing, but also in the CRTM itself) are done in frequency units of cm^{-1}.

1.2 Computation of polychromatic correction coefficients

In the CRTM, the conversion of *channel resolution* radiances to brightness temperatures has to take the passband widths into account. For any channel, the regression relation to be solved is

$$a_0 + a_1 T + \ldots = \frac{k_1}{\ln\left[\dfrac{k_2}{R(T)} + 1\right]} = Y(T) \tag{1.2}$$

where

$$\begin{aligned} T &= \text{brightness temperature} \\ a_j &= \text{regression coefficients} \\ k_1, k_2 &= \text{Planck coefficients} \\ R(T) &= \text{channel radiance} \\ Y(T) &= \text{“effective” brightness temperature} \end{aligned} \tag{1.3}$$

and the channel radiances used to determine the effective temperatures, $Y(T)$, are computed the usual way

$$R(T) = \frac{\int B(T,\nu)\, \phi_{rel}(\nu)\, \mathrm{d}\nu}{\int \phi_{rel}(\nu)\, \mathrm{d}\nu} \tag{1.4}$$

The quantity minimised to obtain the a_j coefficients is

$$\left[\sum_{j=0}^{M} a_j T_i - Y(T_i)\right]^2 \quad \text{for} \quad T_i = 150K, \ldots, 340K \ \text{ in 5K steps.} \tag{1.5}$$

Currently the number of coefficients is fixed at two (i.e. $M = 1$).

2 Summary

2.1 SRF processing

The following tables list the computed central frequencies and polychromatic correction coefficients for the two platforms - with the visible/near-infrared and thermal infrared channels shown in the same table. The thermal infrared channel (7-16) temperature fit residuals for Himawari-8 and Himawari-9 are shown in appendix C and D respectively.

2.1.1 Himawari-8 AHI results

Table 2.1: The computed Himawari-8 AHI channel central frequencies and polychromatic correction coefficients.

AHI Channel	ν_0 (cm^{-1})	a_0 (offset) (K)	a_1 (slope) (K/K)
1	21292.017360	9.20404511	0.99855531
2	19631.143232	4.69013341	0.99921121
3	15715.348991	12.45956928	0.99747041
4	11679.231796	0.81169469	0.99977839
5	6212.556736	-0.08600138	0.99998588
6	4431.783786	-0.12315964	1.00001516
7	2575.766201	0.46831456	0.99932532
8	1609.247001	1.62994353	0.99648350
9	1442.073358	0.30715301	0.99926654
10	1361.402851	0.05633627	0.99985885
11	1164.439411	0.13726260	0.99960871
12	1038.109297	0.09313829	0.99970823
13	961.331428	0.09236143	0.99969153
14	890.734490	0.18689627	0.99933458
15	809.237777	0.25679721	0.99900502
16	753.368104	0.06217163	0.99974273

Table 2.2: The difference between the computed Himawari-8 AHI channel central frequencies and polychromatic correction coefficients for the updated SRFs.

AHI Channel	$\Delta\nu_0$ (cm^{-1})	Δa_0 (offset) (K)	Δa_1 (slope) (K/K)
1	-2.948730e+00	-1.932315e-02	2.934937e-06
2	-1.638257e+00	3.233221e-02	-5.461261e-06
3	9.825294e-01	4.180889e-02	-8.290772e-06
4	-1.478858e+00	1.358897e-03	-4.050719e-07
5	3.108371e-01	1.186694e-04	2.564423e-09
6	-1.132725e-01	-7.072453e-05	9.966623e-09
7	-1.724635e-01	2.821625e-03	-4.393341e-06
8	-6.623013e-01	6.659313e-03	-1.506509e-05
9	2.855747e+00	3.847267e-02	-9.091794e-05
10	-5.937431e-01	4.122731e-04	-1.084845e-06
11	-2.966929e-02	3.813717e-04	-1.092369e-06
12	-9.530131e-01	1.159210e-03	-3.866808e-06
13	-1.190341e-01	-1.104039e-03	3.640074e-06
14	-8.199068e-01	6.854955e-04	-2.896825e-06
15	-5.255323e-01	2.479500e-03	-1.024040e-05
16	-7.628907e-01	-2.844491e-04	9.211509e-07

2.1.2 Himawari-9 AHI results

Table 2.3: The computed Himawari-9 AHI channel central frequencies and polychromatic correction coefficients.

AHI Channel	ν_0 (cm^{-1})	a_0 (offset) (K)	a_1 (slope) (K/K)
1	21293.602571	9.22670147	0.99855168
2	19633.574190	4.68136929	0.99921276
3	15700.915266	12.41947505	0.99747654
4	11679.520218	0.81120873	0.99977853
5	6226.573477	-0.08790965	0.99998500
6	4431.429545	-0.12314898	1.00001516
7	2613.624192	0.45363211	0.99936015
8	1607.899911	1.61511907	0.99651598
9	1438.938969	0.26905376	0.99935665
10	1361.956262	0.05623091	0.99985916
11	1164.300734	0.13393988	0.99961811
12	1039.153196	0.09187536	0.99971243
13	961.332558	0.09414772	0.99968559
14	893.212996	0.18325117	0.99934908
15	810.245068	0.25442415	0.99901536
16	751.672250	0.06218556	0.99974212

3 Impact of updated Himawari-8 AHI SRFs

To determine the impact of the updated Himawari-8 AHI SRFs on the convolved channel radiances, both sets of data (2012 and 2013 SRFs) were convolved with LBL-model generated radiances.

LBLRTM [Clough et al., 2005] v12.2 was used with the ECMWF83 atmospheric profile dataset to generate radiance spectra. The radiance spectra were convovled with the SRFs to yield channel resolution radiances which were then converted to brightness temperatures for each SRF set. The statistics of the brightness temperature differences for the Himawari-8 AHI are shown in figure 3.1. The largest brightness temperature differences occur for channels 9, 10, 12, and 16. Inspection of the SRFs indicate those differences are due to SRF width changes (channel 9, see figure A.3) and SRF shifts (channels 10, 12, and 16; see figures A.4 and A.6).

Figure 3.1: Statistics of the brightness temperature differences between the original 2012 and updated 2013 Himawari-8 AHI SRFs. The calculations used LBLRTM v12.2 and the ECMWF83 profile dataset with a surface emissivity of 0.95.

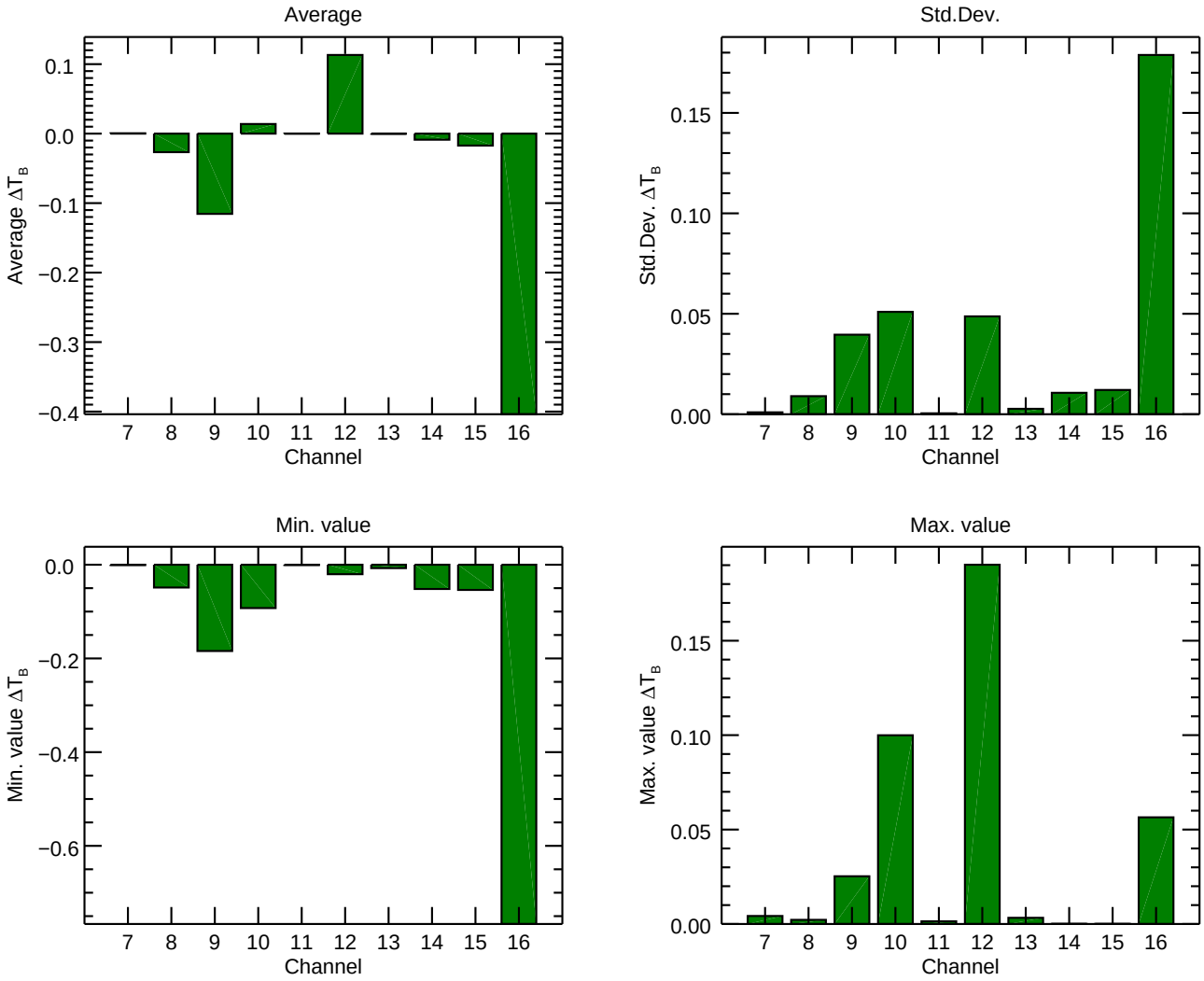

References

S.A. Clough, M.W. Shephard, E.J. Mlawer, J.S. Delamere, M.J. Iacono, K. Cady-Pereira, S. Boukabara, and P. D. Brown. Atmospheric radiative transfer modeling: a summary of the AER codes. *J. Quant. Spectrosc. Radiat. Transfer*, 91:233–244, 2005.

JMA/MSC. Himawari-8 Spectral Response Function (SRF) Data, Sept. 2013a. URL http://www.data.jma.go.jp/mscweb/en/himawari89/space_segment/srf_201309/AHI-08_SpectralResponsivity.zip. Accessed: 2016-02-22.

JMA/MSC. Himawari-9 Spectral Response Function (SRF) Data, Oct. 2013b. URL http://www.data.jma.go.jp/mscweb/en/himawari89/space_segment/srf_201310/AHI-09_SpectralResponsivity.zip. Accessed: 2016-02-22.

A Himawari-8 AHI SRF Data Plots

Figure A.1: Himawari-8 AHI channels 1-3 responses. Vertical dashed lines are the locations of the computed central frequencies. **(Left)** Linear y-axis. **(Right)** Base-10 logarithmic y-axis.

Channel 1

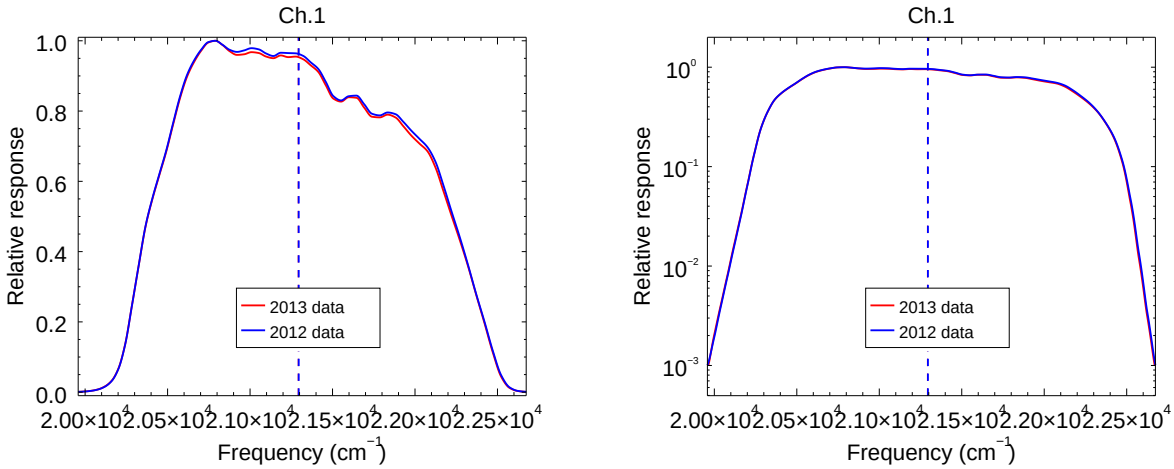

Channel 2

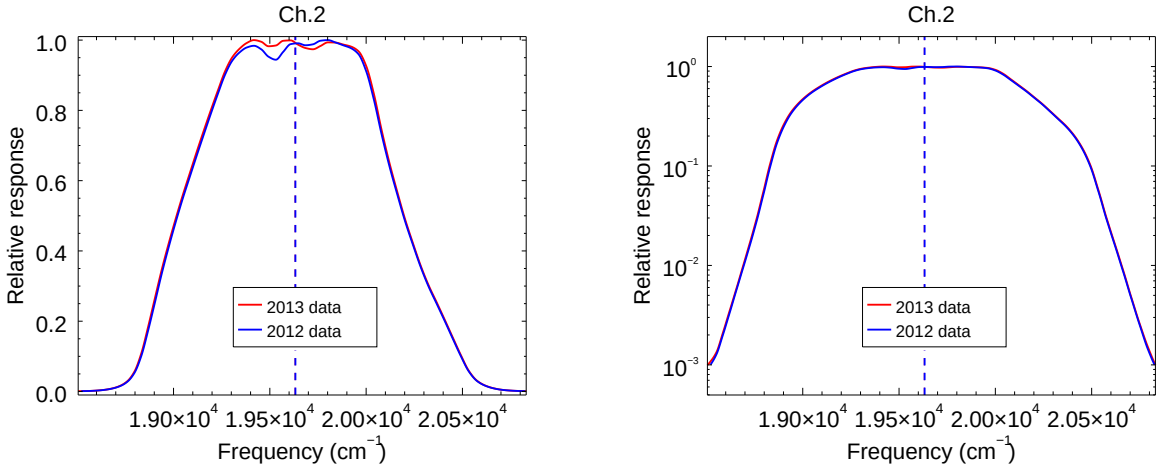

Channel 3

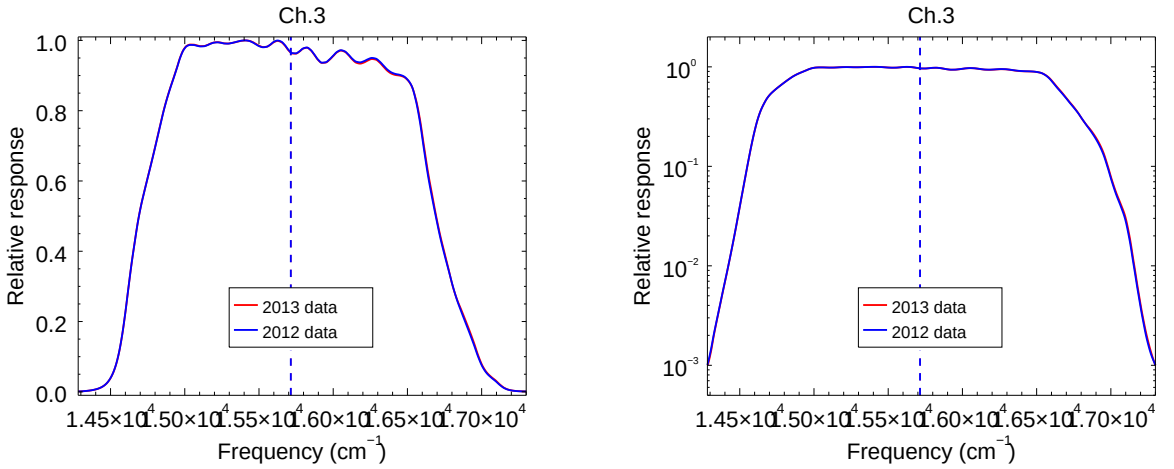

Figure A.2: Himawari-8 AHI channels 4-6 responses. Vertical dashed lines are the locations of the computed central frequencies. **(Left)** Linear y-axis. **(Right)** Base-10 logarithmic y-axis.

Channel 4

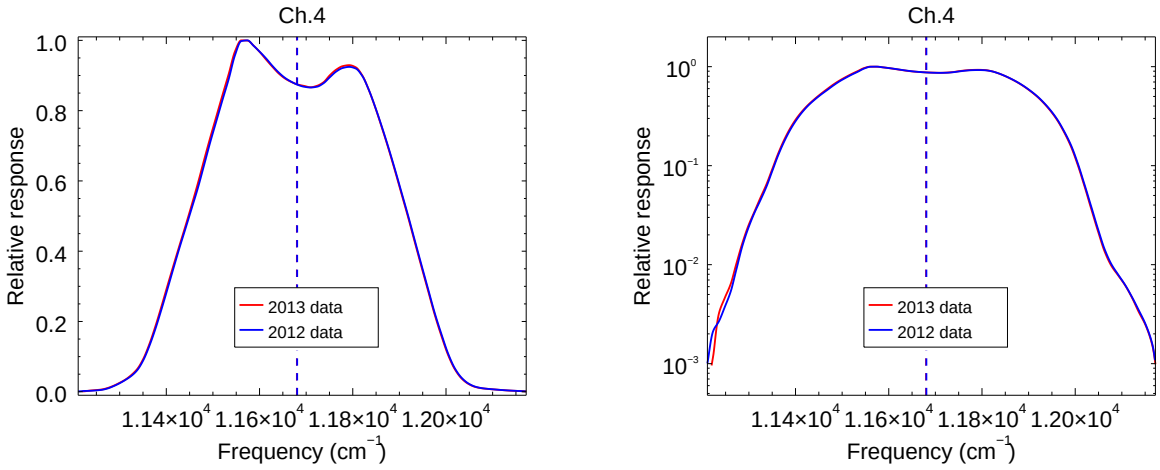

Channel 5

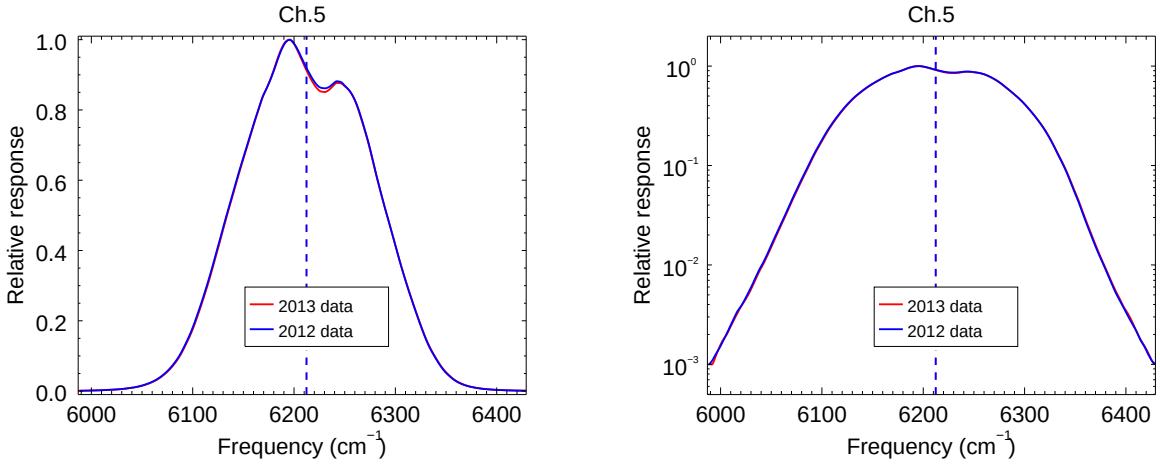

Channel 6

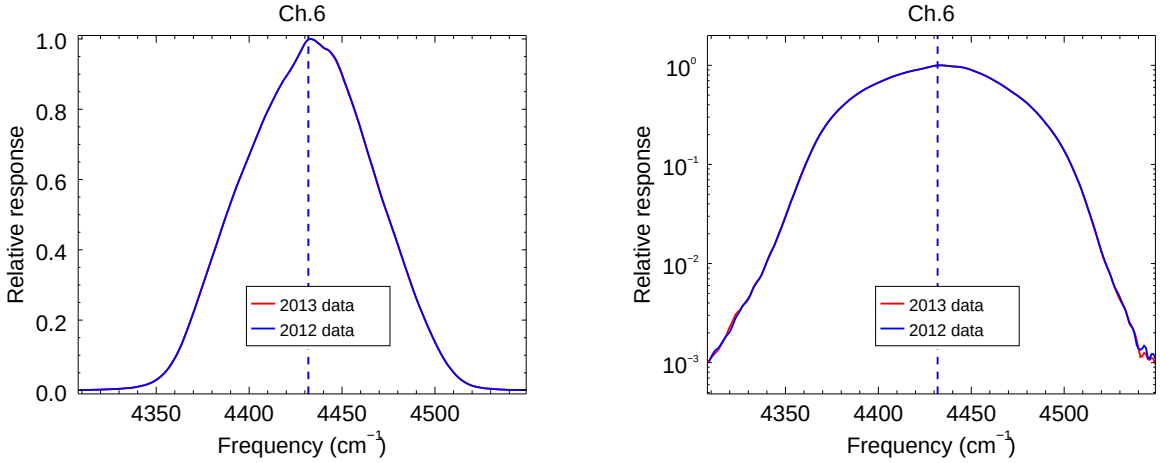

Figure A.3: Himawari-8 AHI channels 7-9 responses. Vertical dashed lines are the locations of the computed central frequencies. **(Left)** Linear y-axis. **(Right)** Base-10 logarithmic y-axis.

Channel 7

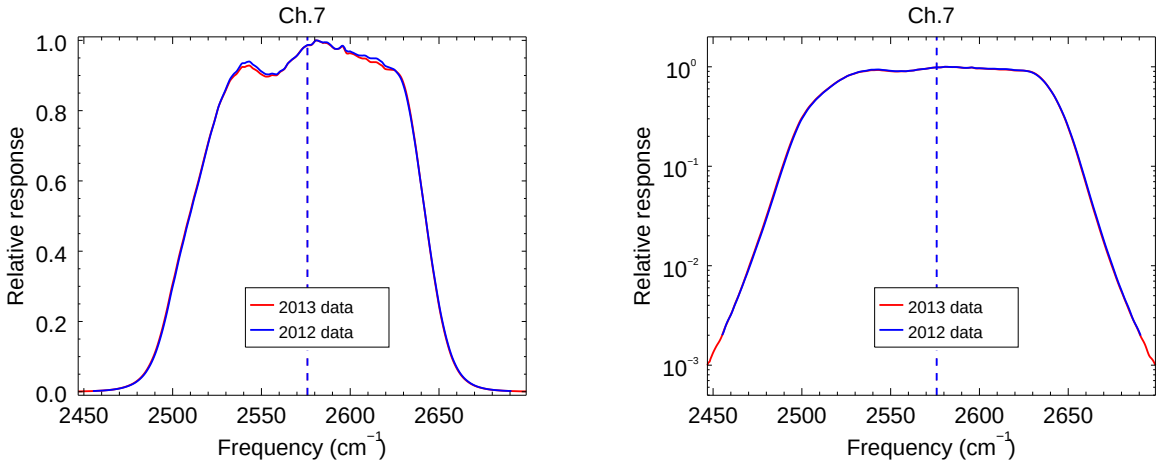

Channel 8

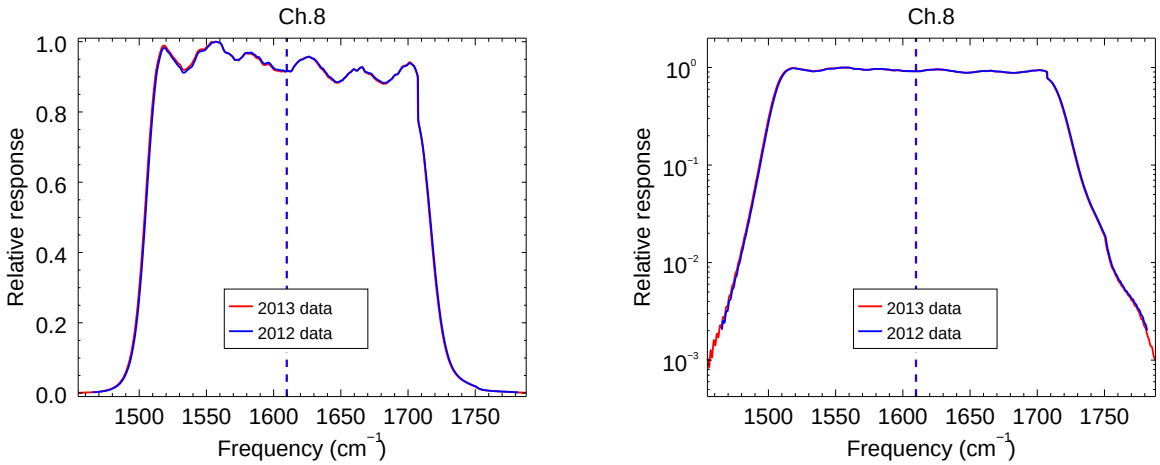

Channel 9

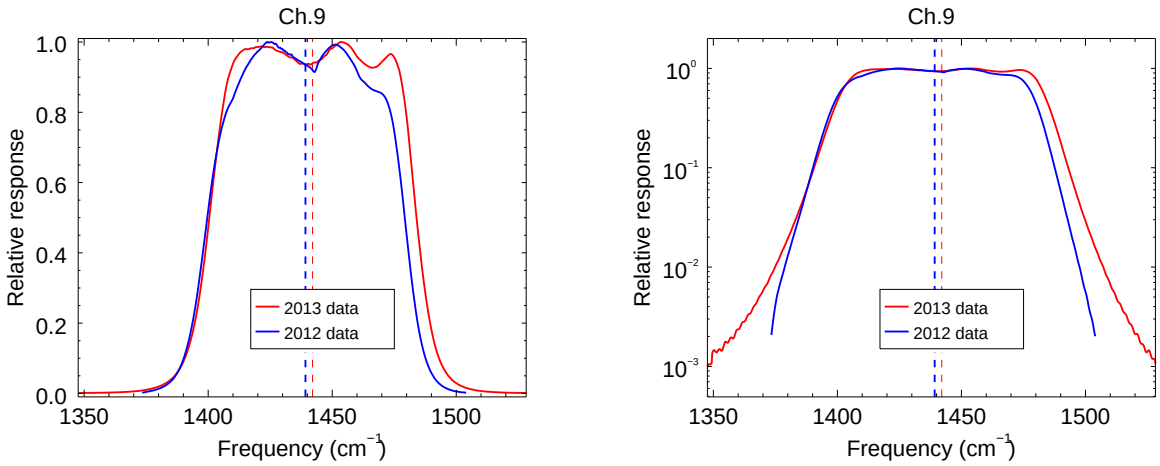

Figure A.4: Himawari-8 AHI channels 10-12 responses. Vertical dashed lines are the locations of the computed central frequencies. **(Left)** Linear y-axis. **(Right)** Base-10 logarithmic y-axis.

Channel 10

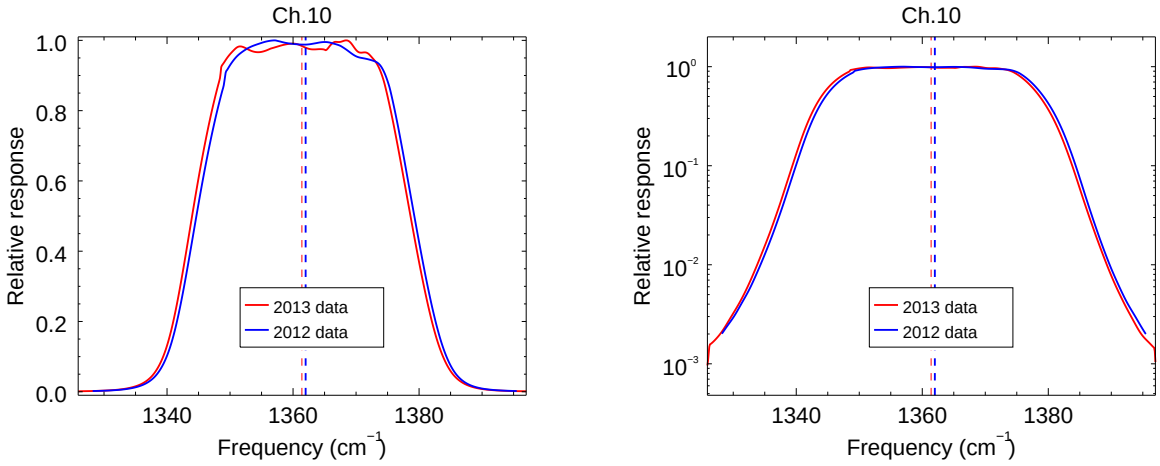

Channel 11

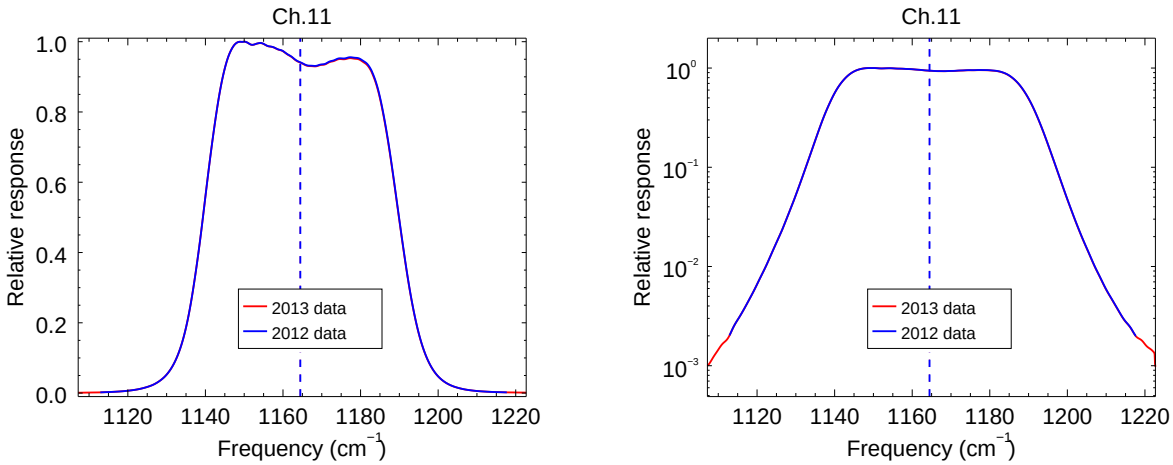

Channel 12

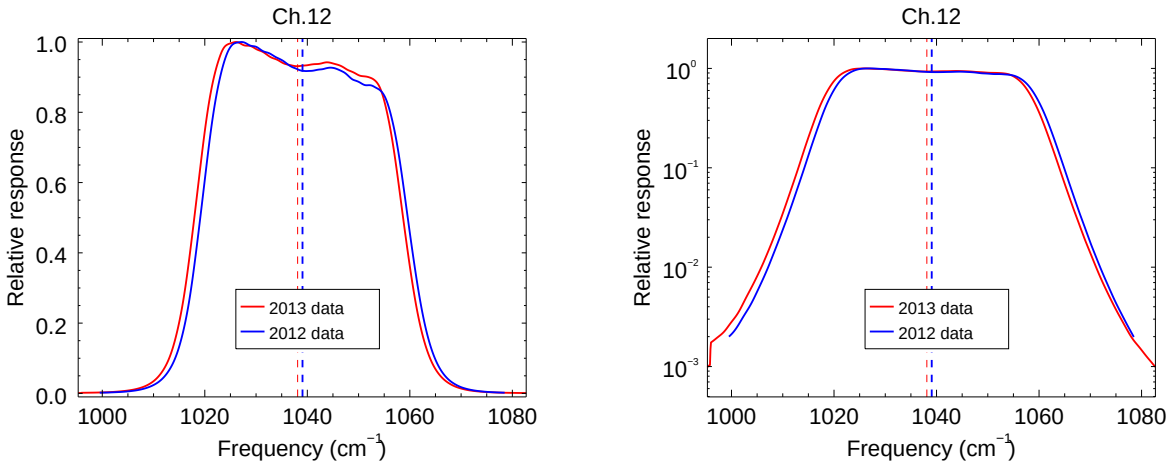

Figure A.5: Himawari-8 AHI channels 13-15 responses. Vertical dashed lines are the locations of the computed central frequencies. **(Left)** Linear y-axis. **(Right)** Base-10 logarithmic y-axis.

Channel 13

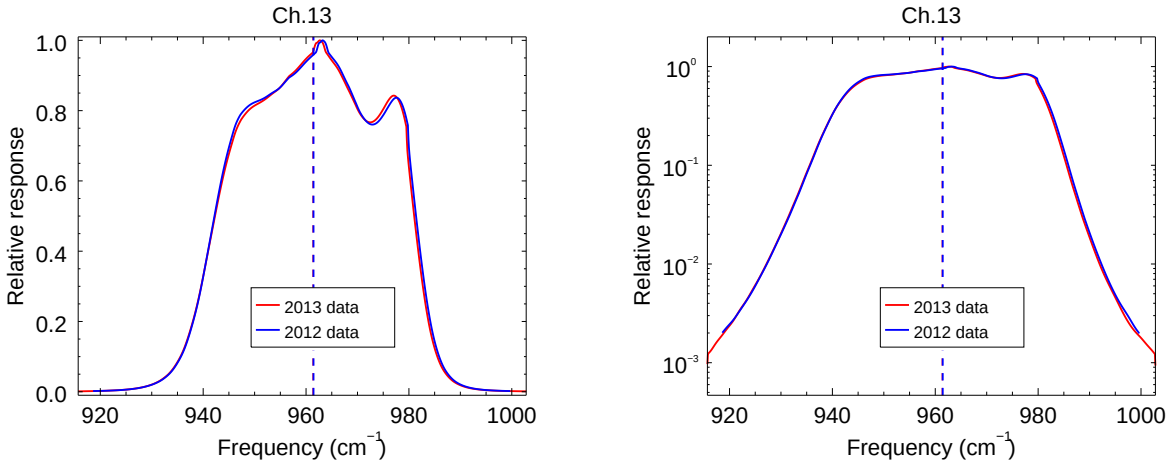

Channel 14

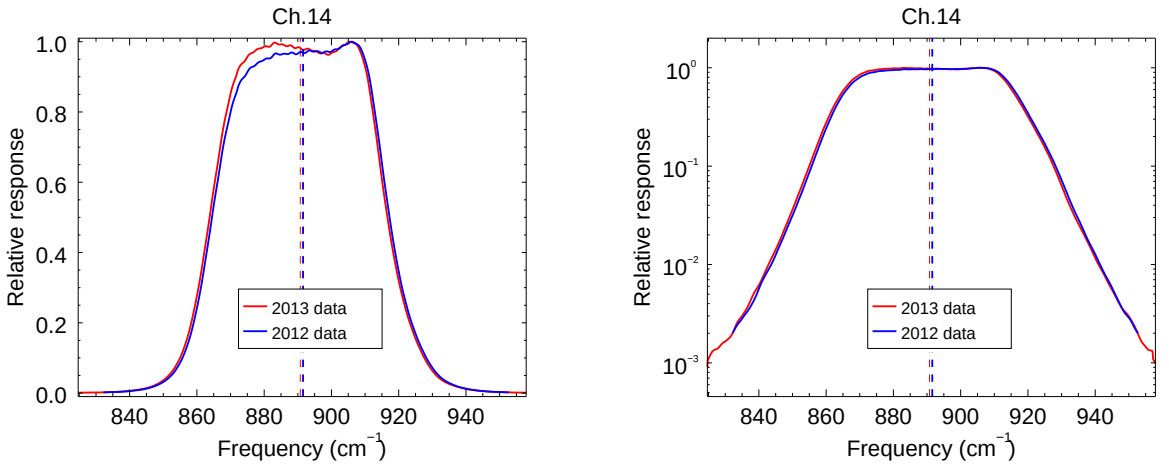

Channel 15

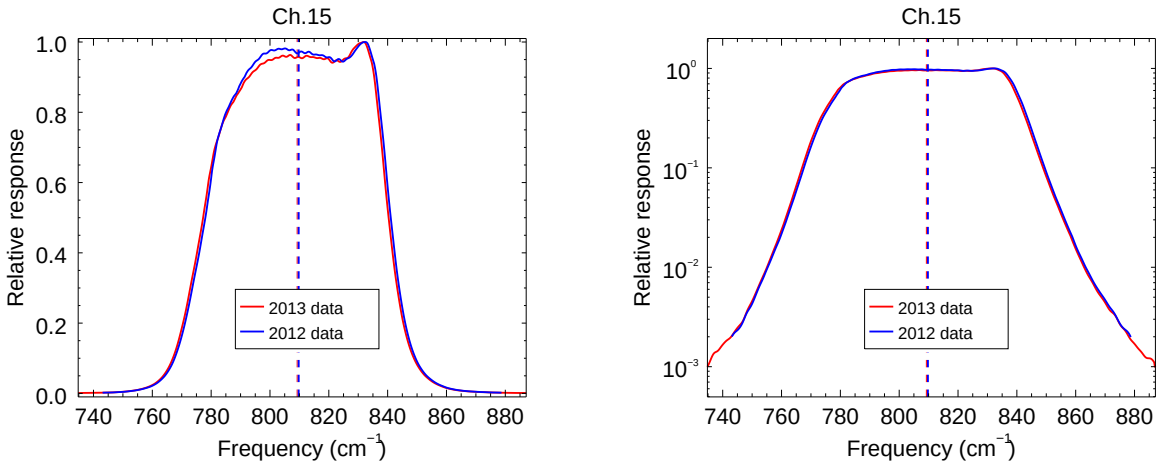

Figure A.6: Himawari-8 AHI channel 16 responses. Vertical dashed lines are the locations of the computed central frequencies. **(Left)** Linear y-axis. **(Right)** Base-10 logarithmic y-axis.

Channel 16

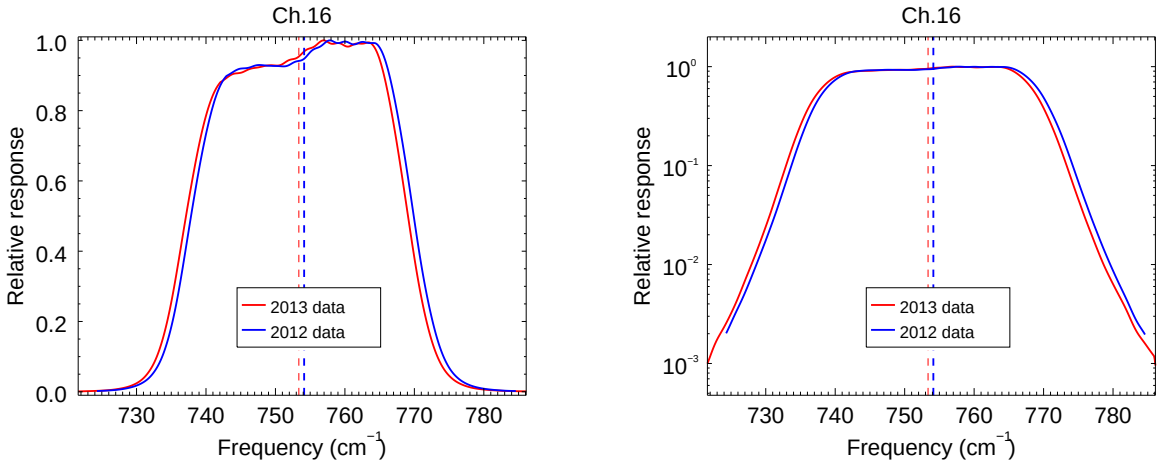

B Himawari-9 AHI SRF Data Plots

Figure B.1: Himawari-9 AHI channels 1-3 responses. Vertical dashed lines are the locations of the computed central frequencies. **(Left)** Linear y-axis. **(Right)** Base-10 logarithmic y-axis.

Channel 1

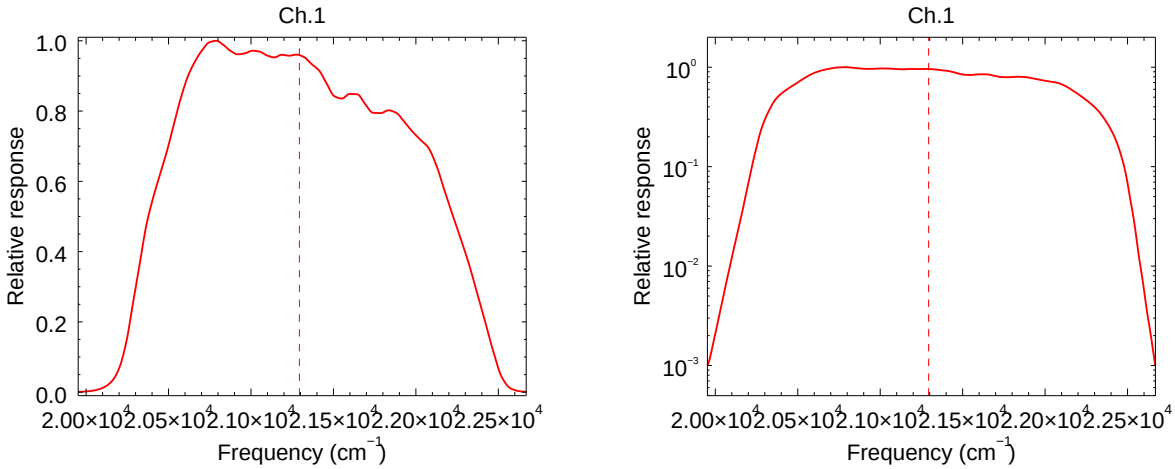

Channel 2

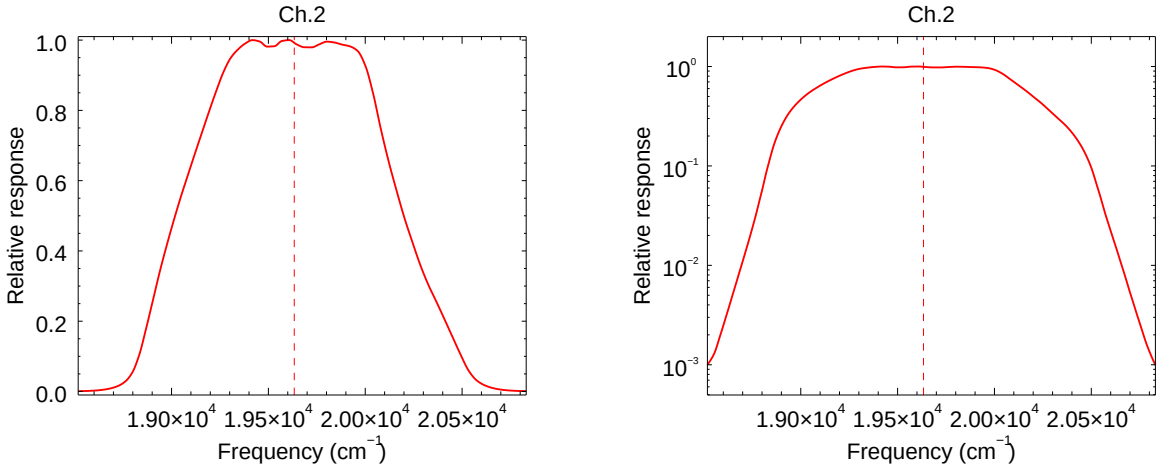

Channel 3

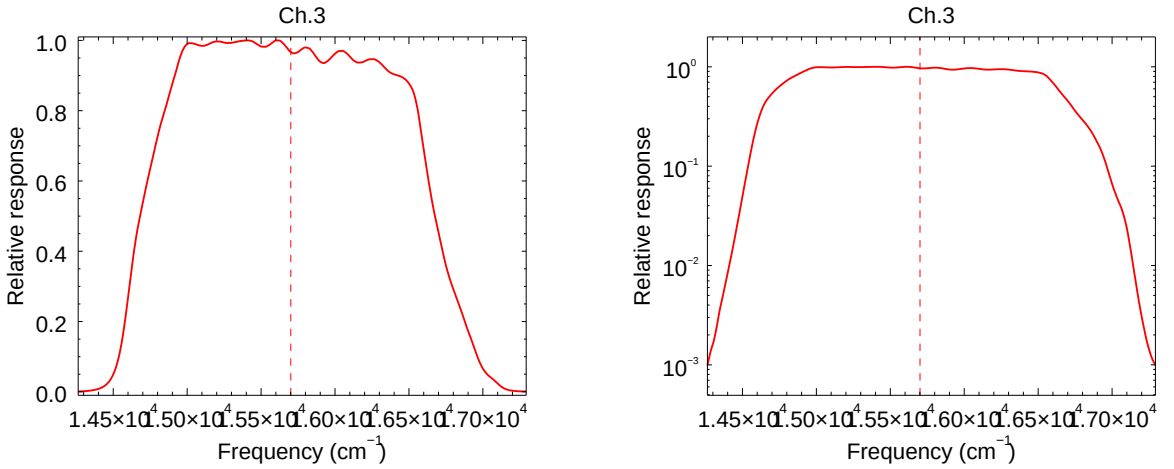

Figure B.2: Himawari-9 AHI channels 4-6 responses. Vertical dashed lines are the locations of the computed central frequencies. **(Left)** Linear y-axis. **(Right)** Base-10 logarithmic y-axis.

Channel 4

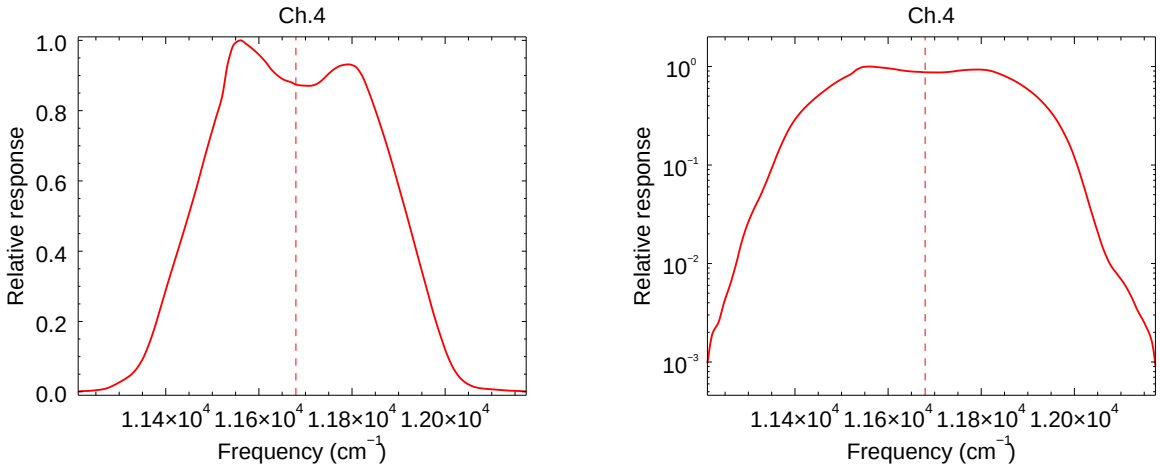

Channel 5

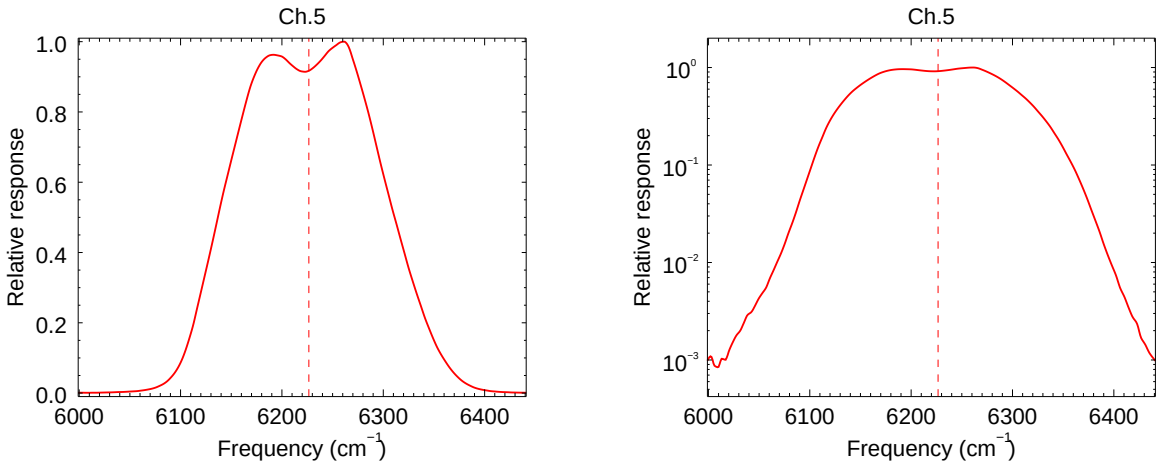

Channel 6

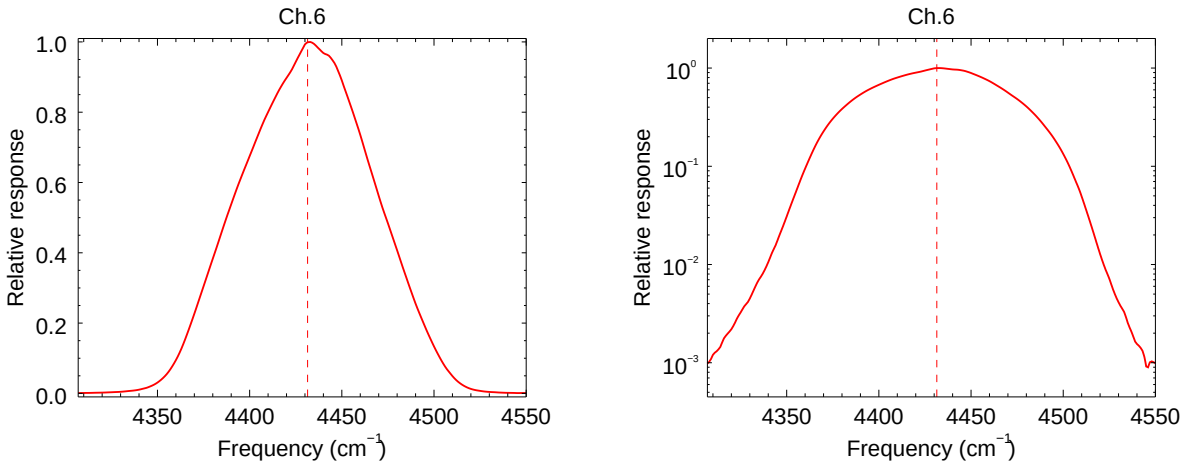

Figure B.3: Himawari-9 AHI channels 7-9 responses. Vertical dashed lines are the locations of the computed central frequencies. **(Left)** Linear y-axis. **(Right)** Base-10 logarithmic y-axis.

Channel 7

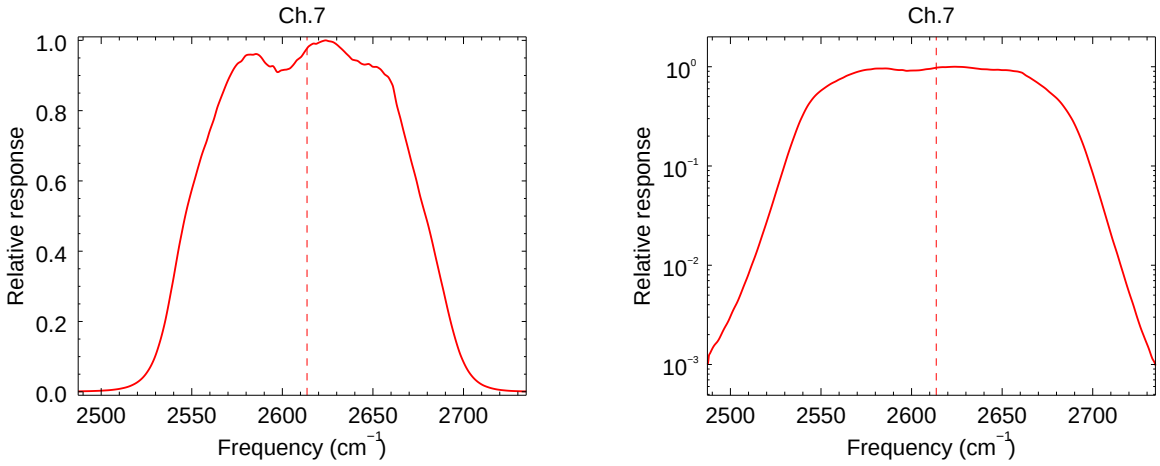

Channel 8

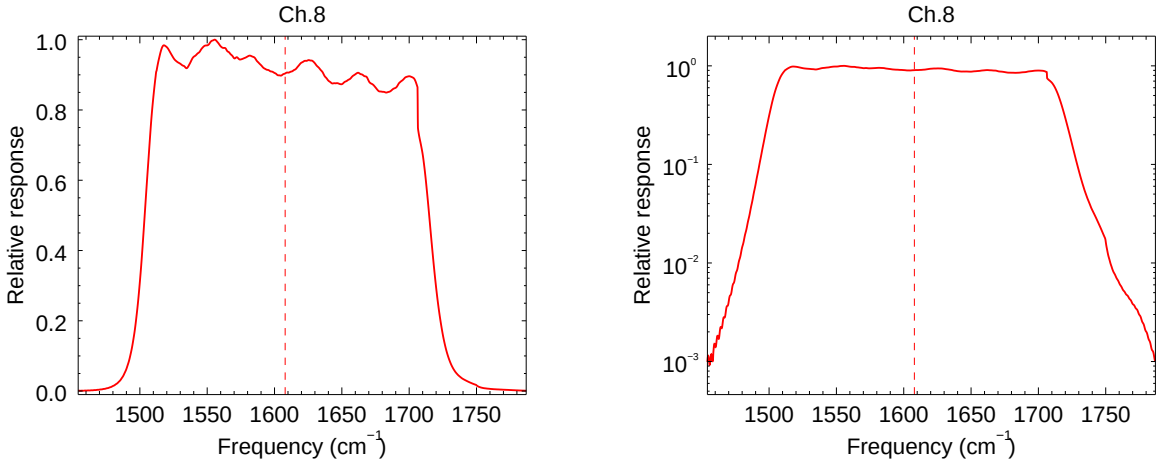

Channel 9

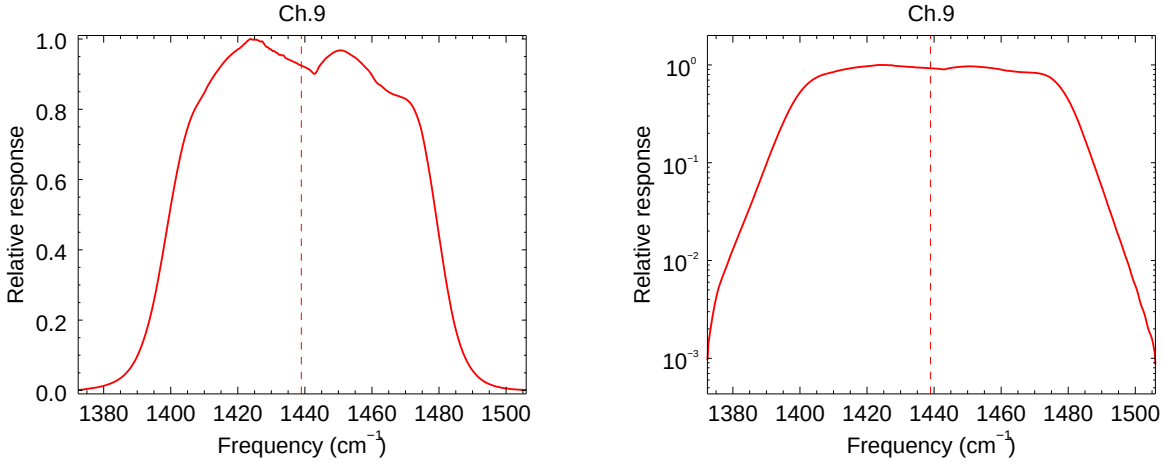

Figure B.4: Himawari-9 AHI channels 10-12 responses. Vertical dashed lines are the locations of the computed central frequencies. **(Left)** Linear y-axis. **(Right)** Base-10 logarithmic y-axis.

Channel 10

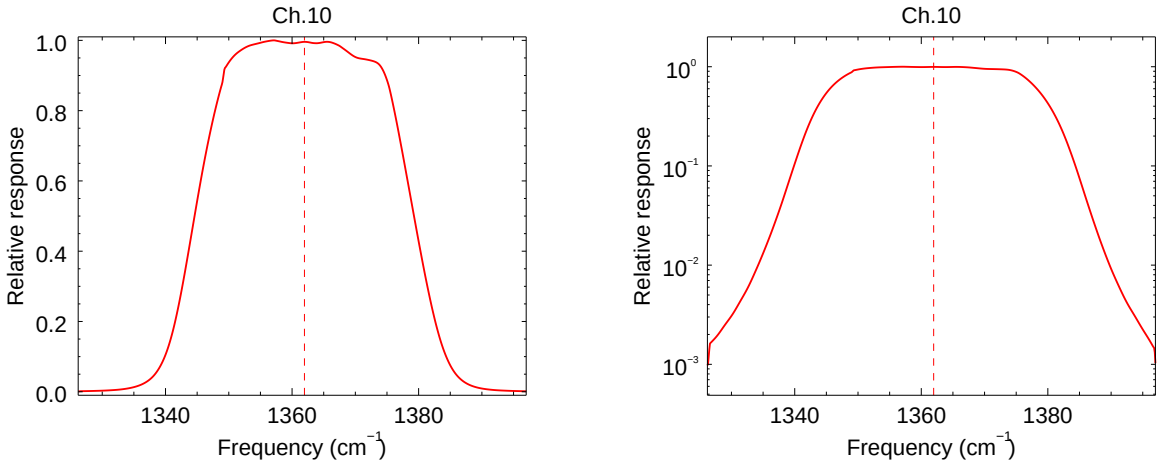

Channel 11

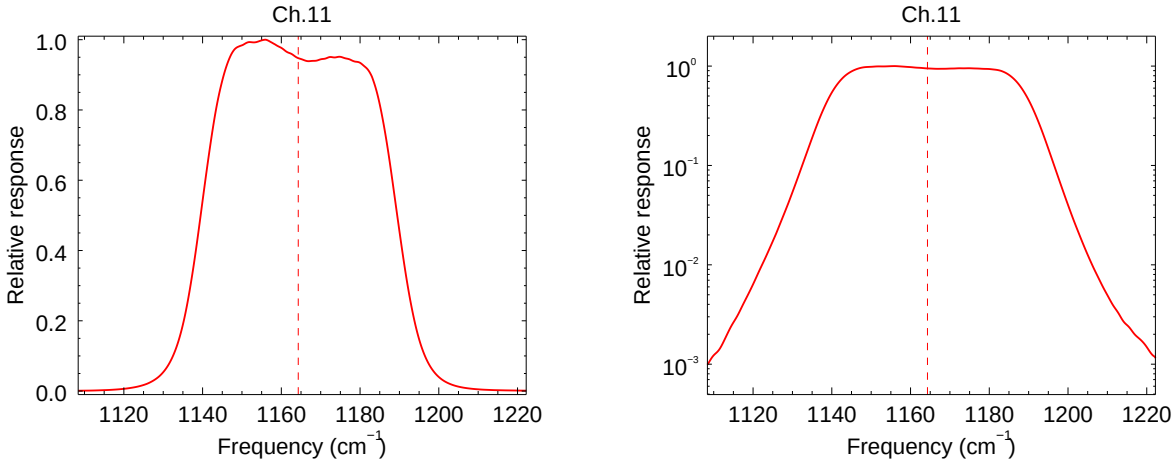

Channel 12

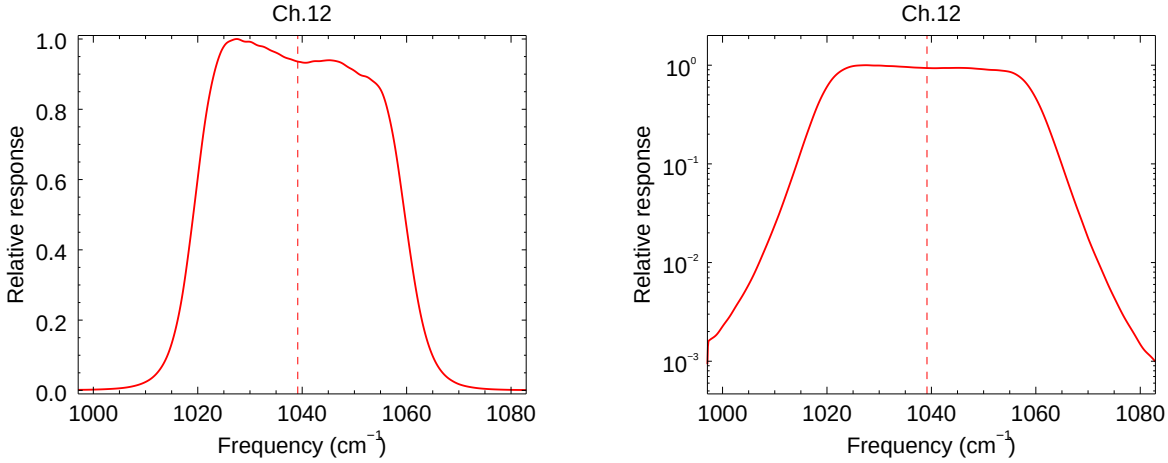

Figure B.5: Himawari-9 AHI channels 13-15 responses. Vertical dashed lines are the locations of the computed central frequencies. **(Left)** Linear y-axis. **(Right)** Base-10 logarithmic y-axis.

Channel 13

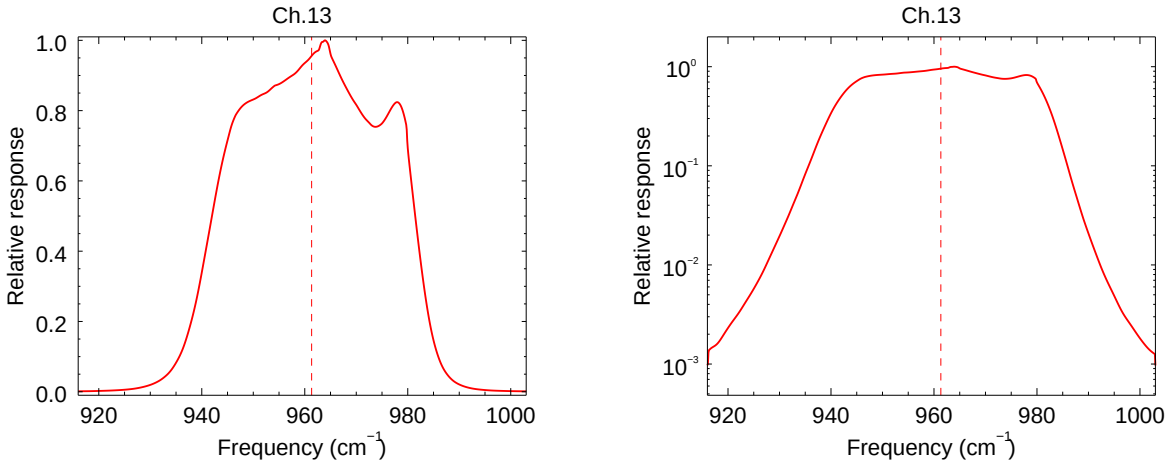

Channel 14

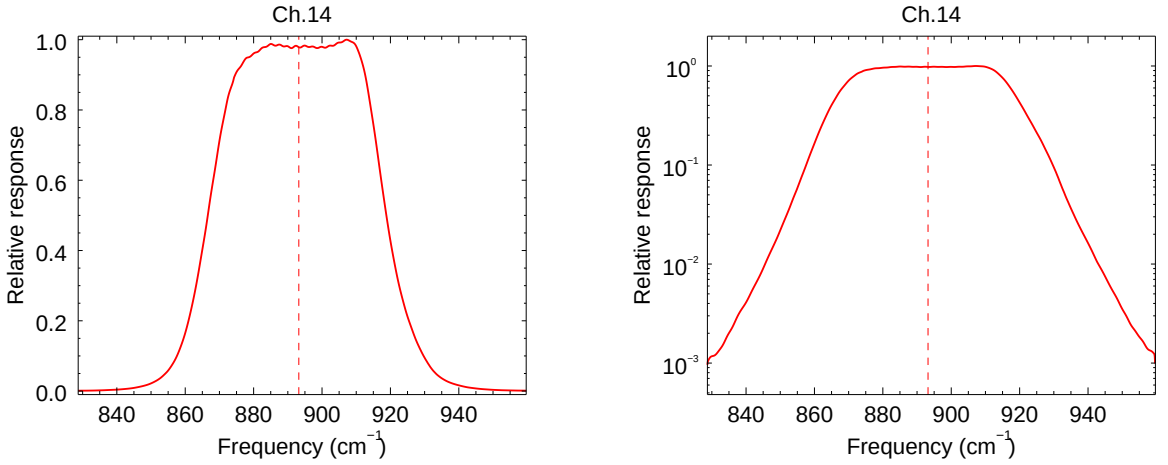

Channel 15

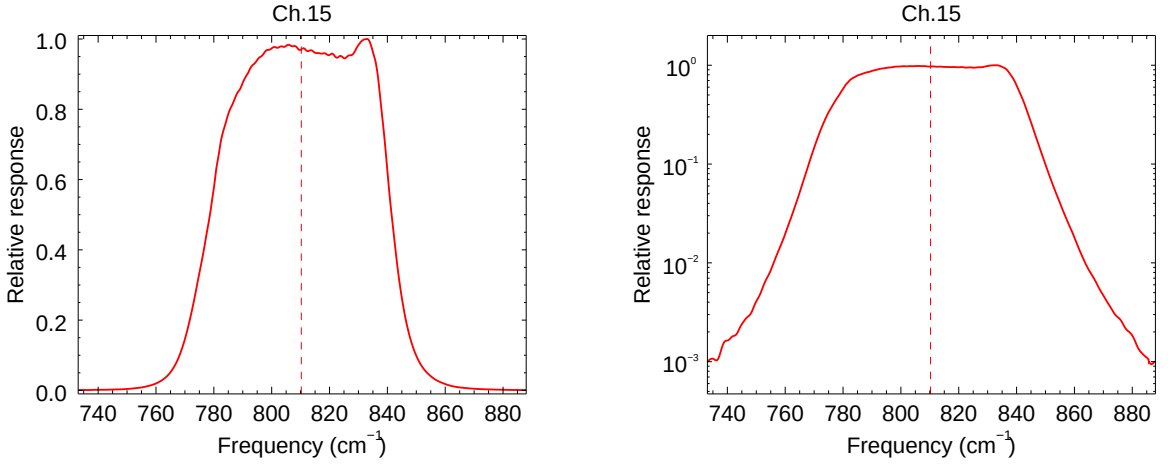

Figure B.6: Himawari-9 AHI channel 16 responses. Vertical dashed lines are the locations of the computed central frequencies. **(Left)** Linear y-axis. **(Right)** Base-10 logarithmic y-axis.

Channel 16

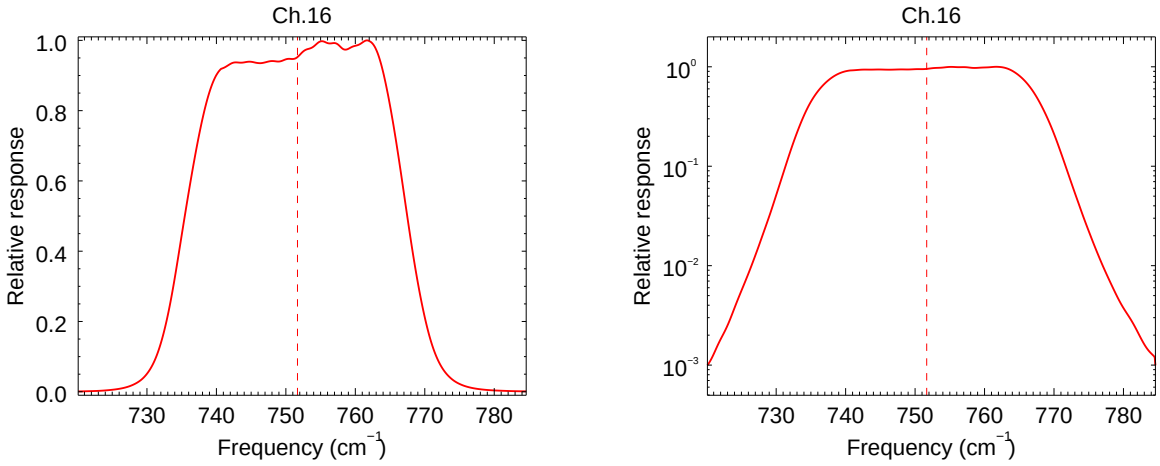

C Himawari-8 AHI Polychromatic Correction Temperature Fit Residual Data Plots

Figure C.1: Himawari-8 AHI channels 7-12 polychromatic correction temperature fit residuals.

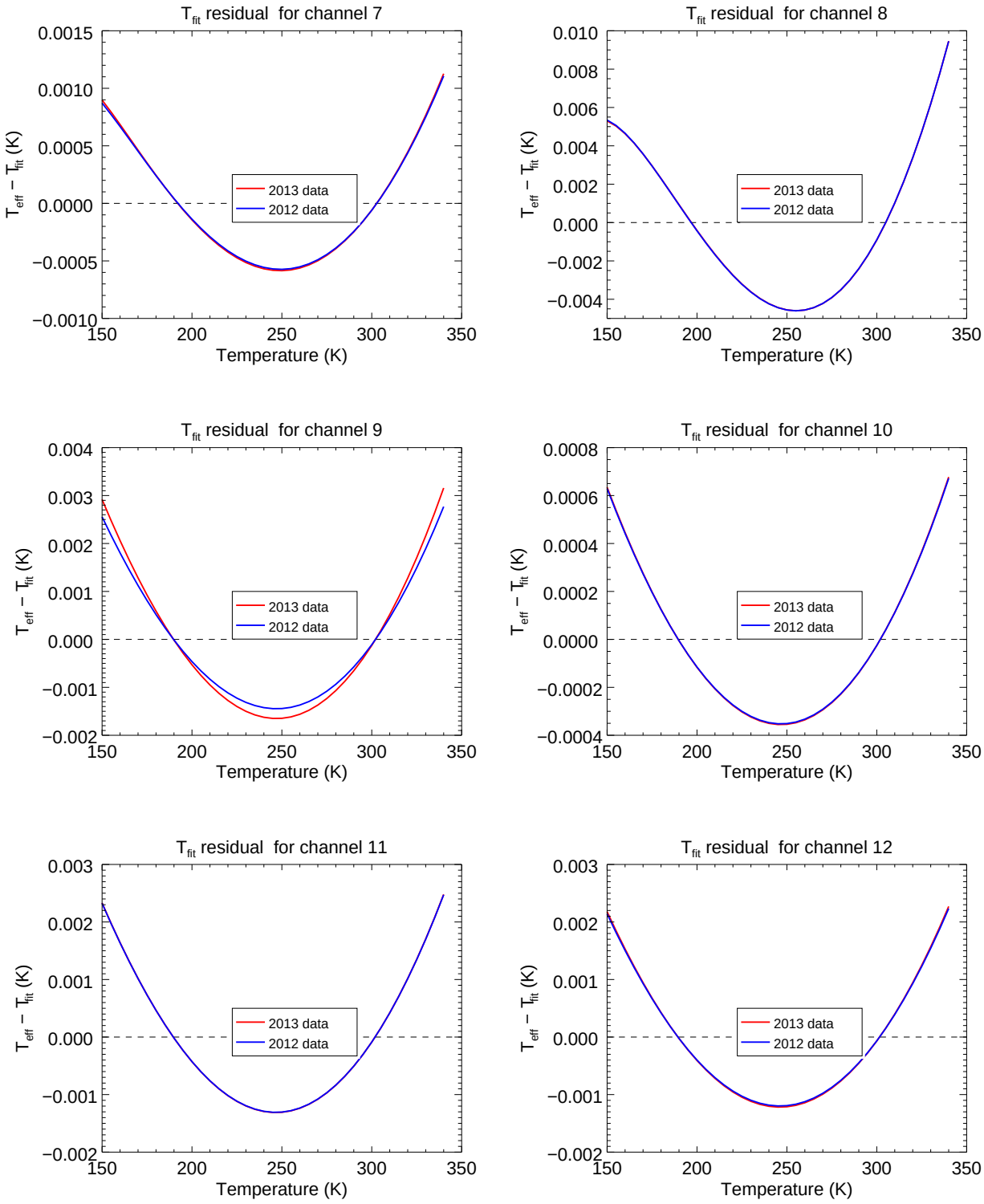

Figure C.2: Himawari-8 AHI channels 13-16 polychromatic correction temperature fit residuals.

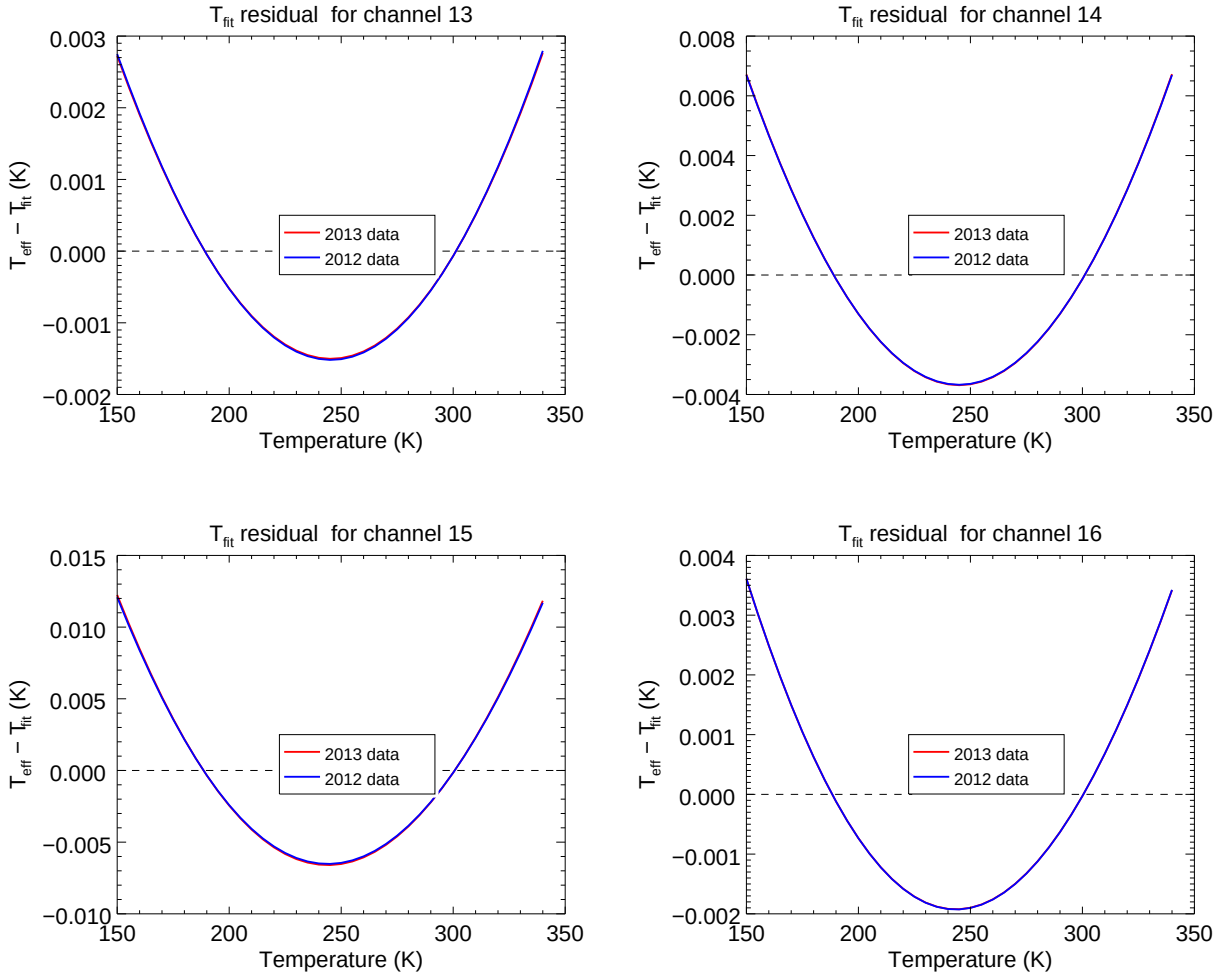

D Himawari-9 AHI Polychromatic Correction Temperature Fit Residual Data Plots

Figure D.1: Himawari-9 AHI channels 7-12 polychromatic correction temperature fit residuals.

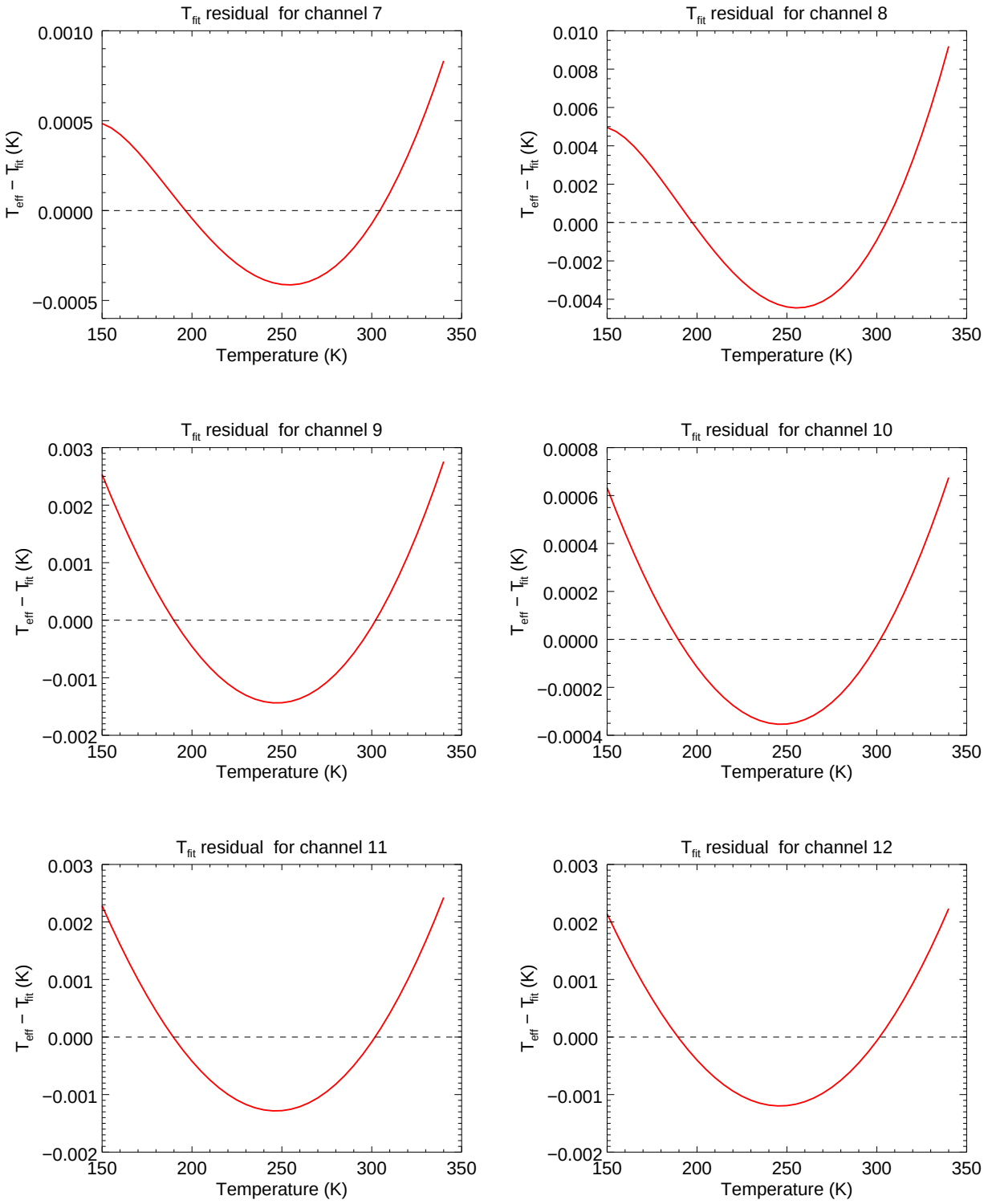

Figure D.2: Himawari-9 AHI channels 13-16 polychromatic correction temperature fit residuals.